PHYSICS OF PLASMAS **21**, 123507 (2014)

Acceleration of neutrals in a nanosecond laser produced nickel plasma

N. Smijesh,[1,2] K. Chandrasekharan,[2] and Reji Philip[1,a)]
[1]*Ultrafast and Nonlinear Optics Lab, Light and Matter Physics Group, Raman Research Institute, Bangalore 560080, India*
[2]*Laser and Nonlinear Optics Lab, Department of Physics, National Institute of Technology Calicut, Calicut 673601, India*

(Received 3 November 2014; accepted 3 December 2014; published online 12 December 2014)

Time of flight dynamics of slow neutrals, fast neutrals, and ions from a nanosecond laser produced nickel (Ni) plasma are investigated. Species arrival times confirm the hypothesis that fast neutrals are formed by the recombination of fast ions with free electrons. Both neutrals and ions are found to accelerate for a short interval immediately after ablation, which is attributed to internal Coulomb forces which create electrostatic potentials resulting in the charged particle acceleration. This process is further enhanced by laser-plasma energy coupling. Emission from neutrals could be measured for longer axial distances in the plume compared to that of ions confirming that the ions recombine to form neutrals as they move away from the target surface. [http://dx.doi.org/10.1063/1.4904308]

INTRODUCTION

Plasmas produced by pulsed lasers are transient in nature. The plasma plume evolves quickly with time after target ablation, and the plume characteristics vary dynamically during expansion. Fundamental studies to understand the dynamics of plume expansion have been of interest to researchers owing to the wide range of applications including pulsed laser deposition,[1] higher harmonic generation,[2,3] production of X-rays[4] and EUV,[5] and nanoparticle and nanocluster generation.[6] Studies such as Optical Emission Spectroscopy (OES), Time of flight (TOF) spectroscopy, Thomson Scattering, Interferometry, Plasma imaging, Langmuir probing, Shadowgraphy, etc., can be used to investigate the properties of laser produced plasmas (LPP). Parameters relevant to the plasma generation and dynamics, such as temperature, number density, plasma frequency, refractive index, etc., can be evaluated using the above mentioned techniques.[7–9] In order to realize a given application, the plasma characteristics may be optimized by tuning the laser energy,[10] wavelength,[11] pulse duration,[12] and nature and pressure of the ambient gas.[13] Target ablation occurs in a few picoseconds after laser irradiation if the pulse intensity equals or exceeds the ablation threshold.[7] The solid target transforms to the gaseous phase forming a high temperature, high pressure, partially ionized gas cloud, during the first few nanoseconds of ablation. This is followed by a rapid expansion leading to the evaporation of neutral atoms, electrons, and ions.[14] The velocity of the plasma front will depend on the incident laser energy and the atomic mass number of the target.[15,16] During the early stages of plume expansion (i.e., in the first few nanoseconds), the inner region of the plasma will be opaque to laser radiation due to its high electron density,[17,18] but it will become transparent when the density falls below a critical value. Therefore, if the laser pulse is several nanoseconds in duration, the energy in the trailing part of the pulse will couple to the plasma electrons, which in turn will drive further ionization of the plasma species via collisional ionization. Besides electron impact ionization, photoionization of species in the plasma by single or multi-photon absorption from the irradiating laser also will lead to the generation of ions. This results in ultraviolet emission (from spontaneous emission of highly excited atoms and ions) and recombination processes, which can also ionize the available neutral atoms.[19]

TOF measurements facilitate the estimation of the velocity of neutral and ionic species in the plasma, which is essential to understand its temporal evolution. The velocity structure of LPP as well as energy and the charge distribution of ions[20,21] can be studied from TOF measurements. It has been calculated that the ion front can be accelerated to velocities which are comparable to the thermal velocities of electrons.[22] While characterizing the properties of laser ablated nanoparticles in high vacuum ($\sim 10^{-7}$ Torr), Amoruso *et al.*[23] has reported the presence of fast neutrals in an ultrafast (300 fs) laser produced nickel plasma at larger laser fluences. Rajeev *et al.*[24] has reported a compact laser-driven plasma accelerator for high energy neutral beams, in which a laser accelerated ion is converted to an energetic neutral atom as a result of highly efficient electron transfer from Rydberg excited clusters. Similarly, our recent studies in ultrafast laser produced zinc and nickel plasmas[25,26] have indicated that fast neutrals indeed accelerate through a short distance along the expansion direction of the plume normal, to the ablation surface. Since the origin of this acceleration required a more detailed investigation, in the present work, we study in detail the occurrence of fast neutrals, their origin, and time of flight dynamics in an LPP generated by irradiating a solid nickel target using a nanosecond laser.

EXPERIMENTAL

Here, a high purity (99.99%) nickel target (ACI alloys, Inc., San Jose) was irradiated using 7 ns, 1064 nm laser pulses which can deliver a maximum energy ∼150 mJ from

[a)]Author to whom correspondence should be addressed. Electronic mail: reji@rri.res.in

an Nd:YAG laser, to produce the plasma. The laser is set to run at 10 Hz for energy stability, but the experiment is performed in the single-shot mode by means of an electronically synchronized fast mechanical shutter positioned in the beam path, which allows only a single pulse to pass through when the shutter is opened. In order to avoid pitting of the target surface, after each laser pulse, the target is moved about 500 μm using a stepper motor driven XY translator, so that the next pulse will irradiate a fresh spot on the target surface. Optical emission spectra in the visible region were recorded using a CCD (Synapse, Horiba Jobin Yvon) attached to the front exit of a high resolution ($\sim$0.06 nm) monochromator (iHR 320, Horiba Jobin Yvon), and spectral lines were identified by comparison with the standard NIST database.[27] The optical TOF (OTOF) spectra of neutrals and ions were recorded by a fast photomultiplier tube (PMT) (R943-02, Hamamatsu) positioned at the side exit of the monochromator. The PMT signal was recorded and digitized using a fast oscilloscope (DPO 7354, Tektronix). By keeping the same laser spot size ($\sim$300 μm) and background pressure (5 Torr, which is the optimum pressure for maximum OTOF signal), measurements were taken for different laser energies to understand the influence of laser fluence on the generation of fast atomic species. After fixing the fluence at approximately 10 J/cm^2 (by focusing $\sim$30 mJ laser pulse using a plano-convex lens of 50 cm focal length on the target surface at an intensity $\sim 1.43 \times 10^9$ W/cm^2), the experiment was repeated for various pressures ranging from 0.05 Torr to 100 Torr, in which emissions from both neutrals and ions were detected. The measurement was repeated for different positions in the plasma plume to calculate the corresponding velocities of ions as well as fast and slow neutrals. In addition, imaging of the plasma was recorded using a lens (Nikon Micro-NIKKOR 55 mm) having a maximum aperture size $f/2.8$ attached to an intensified CCD (ICCD, 4 Picos, Standford Computer Optics, Inc.) positioned perpendicular to the expansion direction of the plasma plume for different pulse energies, for a time delay of 100 ns, employing a gate width of 5 ns. The image recorded by the ICCD is 2X times the actual physical dimension.

RESULTS AND DISCUSSION

Laser ablation occurs within a few picoseconds after target irradiation, and the ablated species interact with the remaining part of the excitation laser pulse. Material ablation occurs once the intensity of irradiation exceeds the ablation threshold of the material, which is given as[7,28]

$$I_{min} = \frac{\rho L_v k^{\frac{1}{2}}}{\Delta t^{\frac{1}{2}}}, \tag{1}$$

where ρ is the density of the material, L_v is the latent heat of vaporization, k is the thermal diffusivity, and Δt is the laser pulse width. I_{min} is calculated to be 3.89×10^8 W/cm^2 for ns excitation, with the corresponding laser fluence being 2.72 J/cm^2 in the present case. Arrival times of ions and neutrals are measured for various laser energies and at different pressures.

OTOF is an effective nondestructive tool to probe the expansion dynamics of various species in the expanding LPP because the technique essentially depends on the detection of emitted radiation. We measured line emissions at 391.6 nm ($3d^9(^2\mathrm{D})\,4p \rightarrow 3d^9(^2\mathrm{D})\,4s$) and 428.5 nm ($3\mathrm{p}^6 3\mathrm{d}^8 (^3\mathrm{P})\,4\mathrm{s} \rightarrow 3\mathrm{p}^6 3\mathrm{d}^9 4\mathrm{s}$) to characterize the expansion dynamics of neutrals (Ni I) and ions (Ni II), respectively. OTOF dynamics measured for energies ranging from 10 mJ to 80 mJ, at a distance of 2 mm on the plasma plumes longitudinal expansion axis normal to the target surface, for 5 Torr nitrogen ambient pressure, are given in Fig. 1. The vertical axis of Fig. 1 is normalized using the maximum voltage recorded on the oscilloscope for the peak P1 for better clarity. At lower laser energies (10 mJ), only a single peak corresponding to slow neutrals (P2) which represent un-ionized neutral species can be seen at a time delay of about 220 ns. At higher energies ($\geq$20 mJ), the OTOF signal of Ni-I displays an additional peak (P1) which occurs at about 80 ns, indicating fast neutrals. The onset of P1 happens earlier with laser energy but that of P2 is unaltered. Ni II displays a single but broader peak (represented as P3 hereafter) for an irradiation energy $\geq$20 mJ. Fast neutrals (P1) and ions (P3) are found to arrive almost at the same delay times indicating that fast neutrals are in fact formed by the recombination of fast ions with electrons.

Fig. 2 displays ICCD images of the expanding LPP recorded for a range of energies from 10 mJ to 80 mJ, measured at 5 Torr nitrogen ambient, for a gate delay of 100 ns and gate width of 5 ns. The presence of two different species moving with different velocities, i.e., a fast moving envelope followed by a relatively slow moving core, can be seen at higher laser energies ($\geq$20 mJ), in agreement with the PMT measurements. The fast and slow species are spatially more separated at higher laser energies, as seen from the ICCD images. The plasma plume expands faster at higher energies: while at 10 mJ the plasma front reaches only up to about 2 mm from the target surface in 100 ns, at 80 mJ it reaches up to about 9 mm. This means the velocity of the plume front increased from 20 km/s to 90 km/s when the irradiation energy increased from 10 mJ to 80 mJ. In short, from the PMT and ICCD measurements it can be understood that P1 and P3 are absent at lower irradiation energies due to the relatively lower number density of ions. At higher energies, these build up concomitantly due to increased ionization via laser-plasma interaction.

For most practical applications, high quality monoenergetic particle beams of electrons, ions, or neutrals produced from laser produced plasma is needed.[29–33] Fast as well as slow ions and neutrals generated along with electrons generated soon after laser ablation moves with different speeds according to their respective thermal energies. Among these, electrons move faster with a velocity V_e, $(=\sqrt{K_B T_e/m_e})$ compared to ions/neutrals due to their larger thermal energy. Since the temperature of plasma is too high soon after ablation, thermal expansion[34] of the plume occur causing positive and negative charges to separate spatially creating a time dependent electric field. This phenomenon slows the electrons that leave the initial volume and ions following them to speed up. Therefore, ions present in the inner region

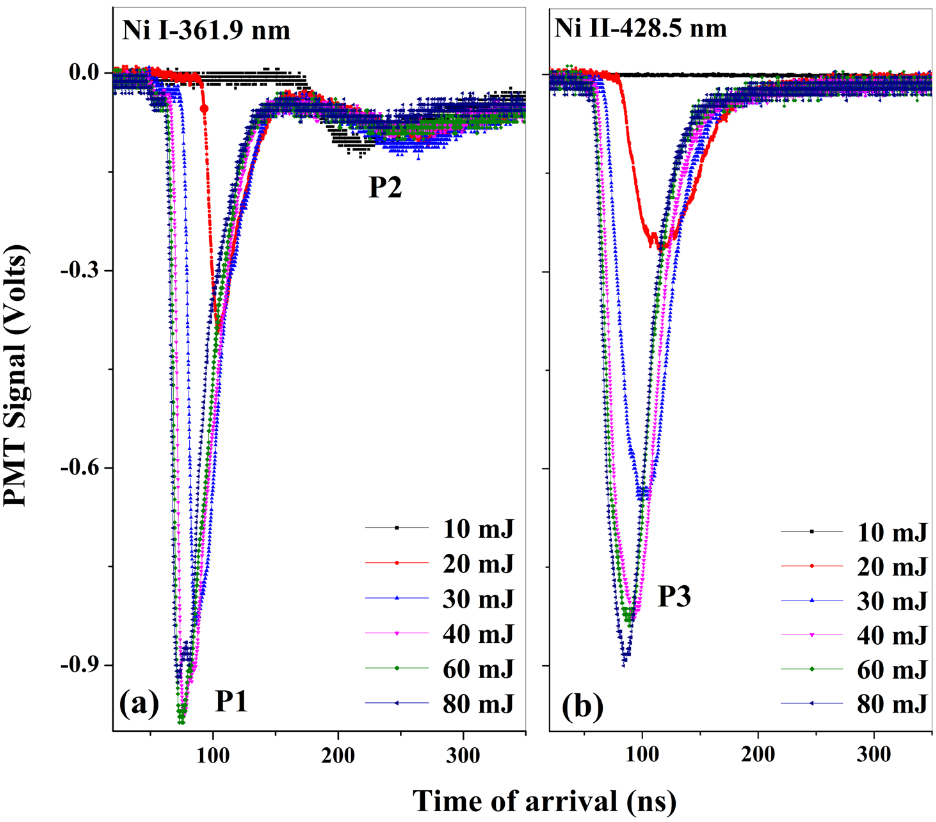

FIG. 1. Time-resolved emission of (a) 361.9 nm ($3d^9(^2D)\ 4p \rightarrow 3d^9(^2D)\ 4s$) transition from Ni I and (b) 428.5 nm ($3p^63d^8\ (^3P)\ 4s \rightarrow 3p^63d^94s$) transition from Ni II, measured in the plasma plume at a distance of 2 mm from the target surface. Ambient pressure is 5 Torr. P1, P2, and P3 represent fast neutrals, slow neutrals, and ions, respectively. Vertical axis is normalized using the maximum voltage recorded on the oscilloscope for the peak P1 for better clarity.

(core) of the plume get accelerated to certain distances at the earlier stages of plasma expansion due to the above mentioned space-charge effect.[35–38] In the present article, an experimental verification on the acceleration of both ions and neutrals occurring to certain distances in an expanding ns laser produced nickel plasma is presented in detail as follows.

Since the nature of the background gas and its pressure will affect LPP expansion dynamics, plasmas can be tuned accordingly for practical applications such as pulsed laser deposition. At lower pressures, the plasma expands adiabatically and the relative scarcity of collisions results in a low number density, leaving more neutrals in the plume. For ns laser pulse irradiation, it is known that the plasma temperature and electron density is enhanced with ambient pressure.[39] The plasma temperature will also increase due to heating via enhanced laser-plasma coupling throughout the plume volume. Indeed the emitted species will interact with

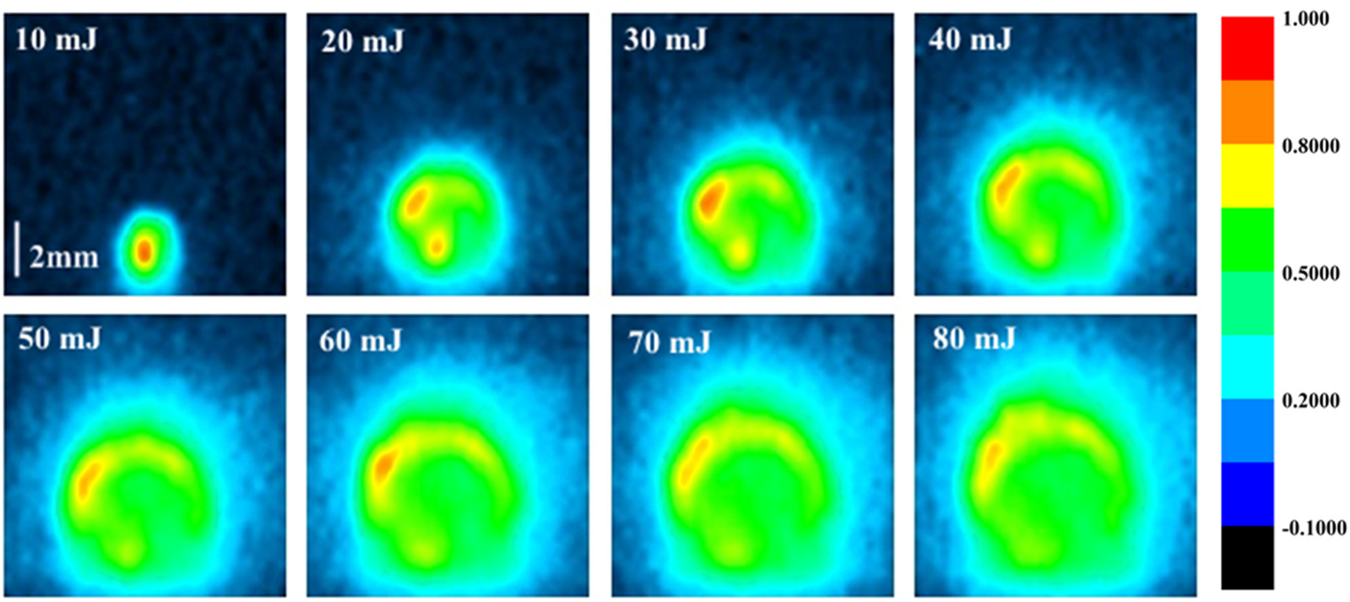

FIG. 2. ICCD images of the expanding plasma plume, measured for laser energies ranging from 10 mJ to 80 mJ. Images are taken 100 ns after the laser pulse hits the target. ICCD gate width is 5 ns, and background gas pressure is 5 Torr. Size of each image window is 11 mm × 11 mm.

the relatively long laser pulse and absorb energy via inverse Bremsstrahlung (IB), the strength of which is given by[40,41]

$$\alpha_{IB} = 1.37 \times 10^{-35}\, \lambda^3 N_e^2 T_e^{-\frac{1}{2}}, \qquad (2)$$

where α_{IB}, λ (μm), and N_e (cm^{-3}) are the IB co-efficient, irradiation wavelength, and electron number density, respectively. The subsequent rise in electron temperature results in enhanced collisions and further ionization. IB enhancement is possible at higher number densities and the confinement generates hotter plasma.[24] At higher pressures, the plasma exhibits a longer history due to plume confinement, but beyond certain optimum pressure plasma temperature and number density will be reduced due to energy loss from collisions with the background gas. This loss mechanism is characterized by the Thermal Leak, given by[23,24]

$$Q_{\triangle t} = \frac{2m_e}{M_B}\, \sigma_{ea} n_B \left[\frac{5kT_e}{\pi m_e}\right]^{1/2}, \qquad (3)$$

where n_B (cm^{-3}) and M_B (kg) are the density and mass of the background gas, respectively, and σ_{ea} is the elastic scattering cross section of the electrons. There exists a certain range of pressures (generally from 10^{-3} Torr to 10^2 Torr) where a relatively large number of density is observed for the plasma species.[23] Accordingly, our measurements were carried out in the pressure range of 5×10^{-2} Torr–1×10^2 Torr.

Species velocities were measured for various positions along the plume axis progressively away from the target surface, until signals from neutrals and ions were too weak to be detected. Results obtained for fast neutrals and ions are shown in Figs. 3(a) and 3(b), respectively. At the lowest pressure used (0.05 Torr), P1 velocity is found to increase from ~20 km/s (at 2 mm) to ~23 km/s (at 4.5 mm), beyond which the signal disappears. At a higher pressure of 1 Torr, P1 accelerates only up to a shorter distance of 3.5 mm (velocity is 25 km/s at 2 mm and 32 km/s at 3.5 mm), beyond which it decelerates. The emission is observed until 7.5 mm. This deceleration occurs due to plume confinement, and therefore, the emission can be observed only for shorter axial distances at the higher pressures of 20 Torr and 100 Torr. From Fig. 3(b), it is seen that at 0.05 Torr the ions accelerate and fly away without being detected beyond 4.5 mm. At 1 Torr, ion velocity increases from 27 km/s to 30 km/s for a movement of 2 mm (from the 2 mm to 4 mm position) along the plume axis. At larger distances (after 4 mm), ions decelerate due to the reduced coulomb pull, though emission can still be detected up to 8.5 mm. At 20 Torr and 100 Torr, the OTOF signal is very weak beyond the 4 mm and 3 mm positions, respectively, which is possibly due to a higher rate of recombination. From Figs. 3(a) and 3(b), it can be seen that the plume length is largest for 1 Torr ambient pressure.

From these results it becomes clear that acceleration of fast neutrals and ions can indeed be observed in expanding nanosecond laser produced plasmas at relatively higher input fluences. Ion acceleration occurs due to the internal electrostatic fields generated by space charges present in the plume, and also due to laser-plasma energy coupling. Ion velocity is reduced at larger distances due to the reduced number density. The experimental observation that fast neutrals are accelerating in a ns LPP for certain optimized conditions of background pressure and laser fluence is novel. The measured acceleration of fast neutrals and ions is consistent when the experiment is repeated for various axial distances and pressures. From the measured arrival times of neutral and ionic species, it is experimentally confirmed that recombination of fast ions with electrons during plasma expansion is the primary mechanism for the generation of fast neutrals in the present LPP. This recombination mechanism was proposed earlier by Amoruso *et al.*[23] in the context of an ultrafast (femtosecond) Ni LPP expanding into a near-vacuum background of 10^{-7} Torr, but has not been experimentally verified yet.

Fig. 4 shows the velocities of slow neutrals measured at the pressures of 0.05 Torr, 1 Torr, 20 Torr, and 100 Torr, for

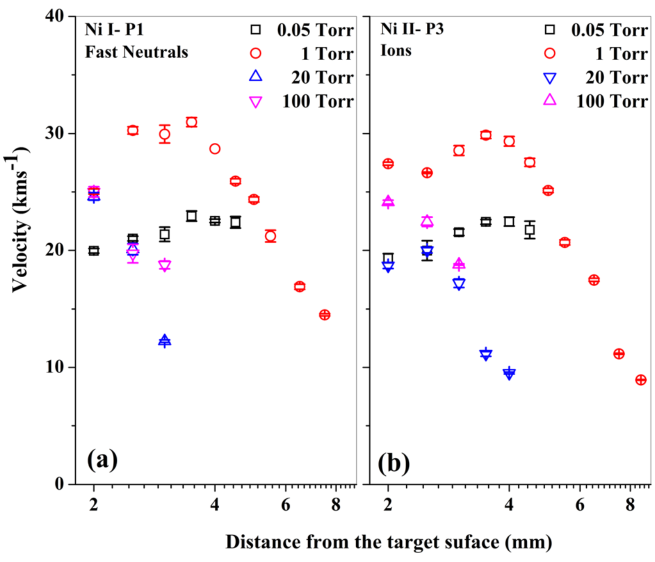

FIG. 3. Velocities of the (a) fast Ni I atomic species and (b) Ni II ionic species, measured at various axial distances from the target surface, for a range of ambient pressures. Maximum velocity is seen at 1 Torr. Laser pulse energy is 30 mJ. Error is calculated using multiple measurements.

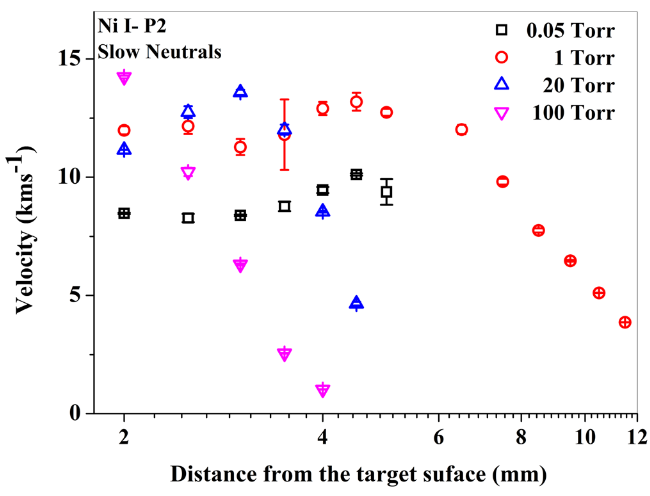

FIG. 4. Velocities of slow neutrals measured at various axial distances from the target surface, for a range of ambient pressures. Maximum velocity is seen at 1 Torr. Laser pulse energy is 30 mJ. Error bar is derived from multiple measurements.

a laser pulse energy of 30 mJ. Fast neutrals decelerate quickly so that the slow neutrals catch up with them, and the peaks P1 and P2 eventually merge, in between 4 mm and 6.5 mm positions. In this region, fast and slow neutrals cannot be resolved in time and space. The comparatively large error obtained when the measurement is repeated at 3.5 mm is ascribed to the interactions of fast and slow species in the plume causing relatively large shift in the peak of the OTOF signal.

The above measurements conclusively prove that fast neutrals can indeed be generated in nanosecond laser produced plasmas. From the arrival times, it is confirmed that fast neutrals are recombined neutrals produced by the recombination of fast ions with free electrons in the plasma, which is the reason for their initial high velocities. The velocity of fast neutrals and ions increases with the irradiation energy, indicating efficient laser-plasma energy coupling.

CONCLUSION

In summary, a nanosecond laser produced nickel plasma was generated by irradiating a pure solid nickel target with 7 ns laser pulses at 1064 nm. OTOF measurements were performed on the Ni-I (361.9 nm) and Ni–II (428.5 nm) transitions for different ambient pressures, plume axial positions, and laser energies. OTOF peak velocities were measured for various axial positions in the plume. Arrival times of the observed fast neutrals and ions are reduced at higher laser energies, indicating efficient laser-plasma energy coupling. An acceleration of fast neutrals is observed during plume expansion at higher irradiation energies. From the measured species arrival times it is experimentally shown that fast neutrals are generated in the plume by the recombination of fast ions with electrons. This is further confirmed from the observation that fast neutrals decelerate in the later part of plume expansion and co-propagate with the slow neutrals.

ACKNOWLEDGMENTS

The authors are grateful to Professor Ajai Kumar and Mr. Jinto Thomas of the Institute for Plasma Research, Gandhinagar, for access to the ICCD unit.

[1]D. H. Lowndes, D. B. Geohegan, A. A. Puretzky, D. P. Norton, and C. M. Rouleau, Science **273**, 898 (1996).
[2]C. Thaury and F. Qu′er′e, J. Phys. B: At., Mol. Opt. Phys. **43**, 213001 (2010).
[3]R. A. Ganeev, J. Phys. B: At., Mol. Opt. Phys. **40**, R213 (2007).
[4]C. Chenais-Popovics, O. Rancu, P. Renaudin, and J. C. Gauthier, Phys. Scr. **T65**, 163 (1996).
[5]D. D. Burgees, B. C. Fawcett, and N. J. Peacock, Proc. Phys. Soc. **92**, 805 (1967).
[6]S. Amoruso, G. Ausanio, R. Bruzzese, M. Vitiello, and X. Wang, Phys. Rev. B **71**, 033406 (2005).
[7]D. A. Cremers and L. J. Radziemski, *Handbook of Laser Induced Breakdown Spectroscopy* (John Wiley & Sons Ltd., 2006).
[8]C. Phipps, *Laser Ablation and Its Applications* (Springer Science & Business media LLC, 2007).
[9]D. W. Hahn and N. Omenetto, Appl. Spectrosc. **64**(12), 335A–366A (2010).
[10]S. S. Harilal, R. C. Issac, C. V. Bindhu, V. P. N. Nampoori, and C. P. G. Vallabhan, J. Appl. Phys. **80**, 3561 (1996).
[11]S. S. Harilal, A. Hassanien, D. Campos, P. Hough, and V. Sizyuk, J. Appl. Phys. **109**, 063306 (2011).
[12]B. Verhoff, S. S. Harilal, J. R. Freeman, P. K. Diwakar, and A. Hussanein, J. Appl. Phys. **112**, 093303 (2012).
[13]S. S. Harilal, C. V. Bindhu, M. S. Tillack, F. Najmabadi, and A. C. Gaeris, J. Appl. Phys. **93**, 2380 (2003).
[14]T. Y. Chang and C. K. Birdsall, Appl. Phys. Lett. **5**, 171 (1964).
[15]P. A. H. Saunders, P. Avivi, and W. Millar, Phys. Lett. A **24**, 290 (1967).
[16]R. Sauerbrey, Phys. Plasmas **3**, 4712 (1996).
[17]N. G. Basov, O. N. Krokhin, and G. V. Sklizkov, Appl. Opt. **6**, 1814 (1967).
[18]N. G. Basov, V. A. Gribkov, O. N. Krokhin, and G. V. Sklizkov, Sov. Phys. JETP **27**, 575 (1968).
[19]W. Demtroder and W. Jantz, Plasma Phys. **12**, 691 (1970).
[20]F. E. Ironst, R. W. P. Mcwhirter, and N. J. Peacock, J. Phys. B: At., Mol. Phys. **5**, 1975 (1972).
[21]R. Dinger, K. Rohr, and H. Weber, J. Phys. D: Appl. Phys. **13**, 2301 (1980).
[22]J. E. Crow, P. L. Auer, and J. E. Allen, J. Plasma Phys. **14**, 65 (1975).
[23]S. Amoruso, R. Bruzzese, C. Pagano, and X. Wang, Appl. Phys. A **89**, 1017 (2007).
[24]R. Rajeev, T. M. Trivikram, K. P. M. Rishad, V. Narayanan, E. Krishnakumar, and M. Krishnamurthy, Nat. Phys. **9**, 185 (2013).
[25]N. Smijesh and R. Philip, J. Appl. Phys. **114**, 093301 (2013).
[26]N. Smijesh, K. Chandrasekharan, J. C. Joshi, and R. Philip, J. Appl. Phys. **116**, 013301 (2014).
[27]See http://physics.nist.gov/PhysRefData/ASD/lines_form.html for NIST atomic spectra data base.
[28]L. Moenke-Blankenburg, *Laser Micro Analysis* (John Wiley & Sons Ltd., 1989).
[29]A. Pukhov, Z. M. Sheng, and J. Meyer-ter-Vehn, Phys. Plasmas **6**(7), 2847 (1999).
[30]S. P. Hatchett, C. G. Brown, T. E. Cowan, E. A. Henry, J. S. Johnson, M. H. Key, J. A. Koch, A. B. Langdon, B. F. Lasinski, R. W. Lee, A. J. Mackinnon, D. M. Pennington, M. D. Perry, T. W. Phillips, M. Roth, T. C. Sangster, M. S. Singh, R. A. Snavely, M. A. Stoyer, S. C. Wilks, and K. Yasuike, Phys. Plasmas **7**, 2076 (2000).
[31]X. Zhang, B. Shen, X. Li, Z. Jin, and F. Wang, Phys. Plasmas **14**, 073101 (2007).
[32]L. Yin, B. J. Albright, B. M. Hegelich, K. J. Bowers, K. A. Flippo, T. J. T. Kwan, and J. C. Fernández, Phys. Plasmas **14**, 056706 (2007).
[33]E. L. Clark, K. Krushelnick, M. Zepf, F. N. Beg, M. Tatarakis, A. Machacek, M. I. K. Santala, I. Watts, P. A. Norreys, and A. E. Dangor, Phys. Rev. Lett. **85**(8), 1654 (2000).
[34]A. Maksimchuk, S. Gu, K. Flippo, D. Umstadter, and V. Yu. Bychenkov, Phys. Rev. Lett. **84**(18), 4108 (2000).
[35]V. S. Belyaev, V. P. Krainov, V. S. Lisitsa, and A. P. Matafonov, Phys.-Usp. **51**(8), 793 (2008).
[36]J. H. Whealton and J. C. Whitson, Particle Accelerators **10**, 235 (1980).
[37]V. N. Rai, M. Shukla, and H. C. Pant, Laser Part. Beams **18**, 315 (2000).
[38]A. Bazzani, M. Giovannozzi, P. Londrillo, S. Sinigardi, and G. Turchetti, Comptes Rendus Mécanique **342**, 647 (2014).
[39]N. Farid, S. S. Harilal, H. Ding, and A. Hassanein, J. Appl. Phys. **115**, 033107 (2014).
[40]J. J. Chang and B. E. Warner, Appl. Phys. Lett. **69**, 473 (1996).
[41]P. T. Rumsby and J. W. M. Paul, Plasma Phys. **16**, 247 (1974).